



HAL
open science

Apparatus for the investigation of liquid systems in a shear gradient by small angle neutron scattering (SANS)

P. Lindner, R.C. Oberthür

► **To cite this version:**

P. Lindner, R.C. Oberthür. Apparatus for the investigation of liquid systems in a shear gradient by small angle neutron scattering (SANS). *Revue de Physique Appliquée*, 1984, 19 (9), pp.759-763. 10.1051/rphysap:01984001909075900 . jpa-00245254

HAL Id: jpa-00245254

<https://hal.science/jpa-00245254>

Submitted on 4 Feb 2008

HAL is a multi-disciplinary open access archive for the deposit and dissemination of scientific research documents, whether they are published or not. The documents may come from teaching and research institutions in France or abroad, or from public or private research centers.

L'archive ouverte pluridisciplinaire **HAL**, est destinée au dépôt et à la diffusion de documents scientifiques de niveau recherche, publiés ou non, émanant des établissements d'enseignement et de recherche français ou étrangers, des laboratoires publics ou privés.

Apparatus for the investigation of liquid systems in a shear gradient by small angle neutron scattering (SANS)

P. Lindner (*) and R. C. Oberthür

Institut Laue-Langevin, 156X, 38042 Grenoble Cedex, France

Résumé. — L'utilisation d'un appareillage construit d'après le principe de Couette permet de mesurer la diffusion des neutrons aux petits angles par les liquides soumis à un gradient de cisaillement constant. Lors de cette manipulation on peut mesurer des systèmes typiques, comme des solutions de polymères, des biopolymères anisotropes et des virus en solution ainsi que de nombreuses solutions colloïdales.

Abstract. — A Couette-type apparatus has been constructed which allows the observation of small angle neutron scattering from fluids in a constant shear gradient. Typical systems which can be investigated by this apparatus are polymer solutions and melts, anisotropic biopolymers, viruses in solution and various colloidal liquids.

1. Introduction.

Small angle neutron scattering experiments with liquids have given information about structural properties particularly since intense neutron sources like the ILL high-flux reactor had been available. Measuring the elastic coherent scattering intensity as a function of scattering vector Q we obtain an image in reciprocal space of the distance distribution between the constituent parts of the molecules. Without any external influences the scattering is normally isotropic, being the result of a space and time average over all molecular conformations and orientations. Additional information about the shape and mobility of the molecules is available when the sample experiences orientational forces by a hydrodynamic field during the scattering experiment. The apparatus which is described below allows the study of liquid systems in a hydrodynamic field with constant shear gradient with the two small angle diffractometers of the ILL : D 11 and D 17 [1].

2. Sample container.

The Couette-type sample container is schematically shown in figure 1. It consists of an inner fixed piston (stator) and an outer rotating beaker (rotor), leaving a cylindrical gap which is filled up with the fluid to be investigated. Rotor and stator are both made of

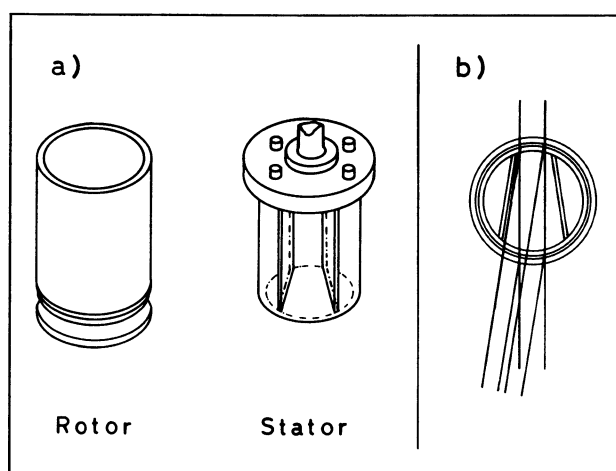


Fig. 1. — a) Schematic view of rotor and thermostatable stator. b) Neutron beam path through the sample included in the gap (1.0 or 0.5 mm) between rotor and stator.

quartz-glass « Suprasil » with excellent optical qualities. The material is highly transparent for thermal neutrons and shows a very low SAS background. The cylinders, manufactured by « HELLMMA » (Müllheim, F.R.G.) have a wall thickness of 2.5 mm, the precision of the inner diameter of the rotor and of the outer diameter of the stator is about $\pm 2 \mu\text{m}$. The stator exists in two versions with different diameters, so that the available cylindrical space has a thickness

(*) Part of PhD-thesis of P. Lindner, at the University of Mainz, F.R.G.

of 1.0 mm or 0.5 mm, depending on the combination of stator and rotor. The height of the gap is 60 mm and the inner diameter of the rotor is 48 mm, the sample volume is therefore $\sim 4.5 \text{ cm}^3$ (gap = 0.5 mm) or $\sim 7.0 \text{ cm}^3$ (gap = 1.0 mm). With the given precision of the diameters, the gap-width varies about $\max \pm 1\%$ over the height of the cylinders.

Laminar flow between the two cylinders is stabilized in this arrangement by centrifugal forces which act on the liquid. When the outer cylinder is rotating, liquid layers near the rotor have a greater velocity than inner ones near the stator. This means, heavier liquid layers are forced towards the outer surface and the system is less perturbed by oscillatory instabilities. The contrary arrangement, where the inner cylinder is rotating (Searle-type) leads even at small flow rates far below the transition to turbulence to so called Taylor-vortices which are superimposed on the laminar flow [2].

Within all stators two compartments beside the beam path are separated. They are connected with an external thermostat and allow the control of the fluid temperature in the range $5^\circ\text{C} \leq T \leq 80^\circ\text{C}$. A Pt-100 resistance element is fixed to the inside of the stator and records the temperature of the gap through the cylinder wall.

The bottom of the stator is formed like a cone, so that the shear gradient is linear in the bottom-gap and approximately equal to the gradient in the annulus. Vortices in the area of the edge are therefore reduced.

The realisation of laminar flow in the range up to the critical rotation speed depends on the Reynolds number Re and on geometrical parameters, i.e. the ratio of the filling height h to the gap-width d , $h/d > 10$, and the ratio of the gap-width d to the cylinder radius R_i , $d/R_i < 0.05$, to assure laminar flow [3]. For both gap-versions is $h/d \geq 50$ and $d/R_i \leq 0.04$ in the case of our apparatus.

The neutron beam of 1.5 cm^2 cross-section hits the apparatus perpendicular to the axis of rotation and passes through both cylinders; it comes therefore twice into contact with the sample volume. On the assumption *a*) that only single scattering is relevant for the experiment and *b*) that the sample-detector distance is great compared with the cylinder diameter, the small angle scattering is in good approximation equal to that of a sample of double thickness $2 \cdot d$, where d is the gap-width and these conditions are fulfilled at the D 11-SANS camera of the ILL. For the operation at the instrument D 17, where experiments are done at greater scattering angles there exists a version with another stator. Both sections of the scattering volume are separated by a set of soller slits on the inside of the stator. The material is covered with gadolinium paint which absorbs neutrons, so that only neutrons scattered from the sample volume near the detector are counted. For both instruments, D 11 and D 17, the range of the scattering vector Q

in reciprocal space is limited by the geometry of the apparatus and the available neutron wavelengths to $10 \mu\text{m}^{-1} \leq Q \leq 2 \text{ nm}^{-1}$.

3. General setup, drive, adjustment.

A schematic view of the central part of the apparatus is shown in figure 2. The rotor is fixed with a screw crap on a brass turn-table. The rotation axis of the table is mounted in three ball-bearings and connected to the axis of a DC-precision motor combined with a tachogenerator (DUNKER-Motor, Bonndorf, F.R.G.).

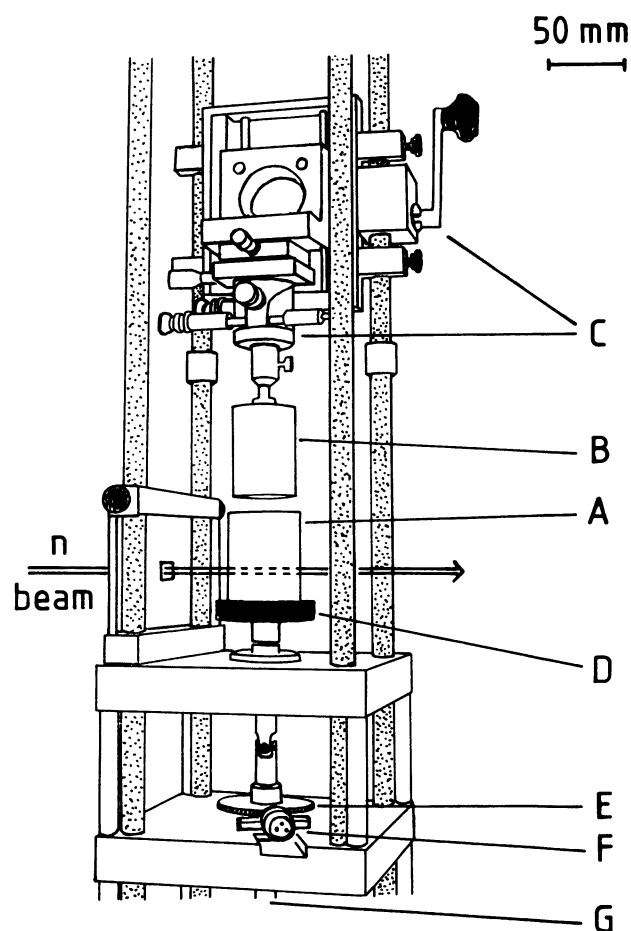


Fig. 2. — Schematic view of the central part of the apparatus. A : quartz-glass rotor, B : stator, C : support for adjustment, D : fixation with screw crap on turn-table, E : rotating cog, F : magnetic detector, G : connection to motor drive (not shown).

The continuous regulation of the motor speed is made by a control unit in a range between $2 \text{ RPM} \leq U \leq 6000 \text{ RPM}$. The rotation speed is detected without mechanical contact by a magnetic detector (AIRPAX) which observes the signal induced by a rotating cog.

The PDP 11-CAMAC system of the SANS instrument controls and regulates the speed during the

measurement so that its variation is at most $\pm 0.5\%$ in the range up to 1 000 RPM and $\pm 1\%$ above this during an operation period of several hours.

The stator is attached to a support (Microcontrolle, Paris, France) so that the axes of the inner and outer cylinder can be adjusted with three linear and two angular motions. The fine correction of the central position of the stator inside the rotor is done manually by adjusting a horizontal meniscus when a low viscosity fluid rotates in the gap.

Drive, cylinder-support and adjustment mechanisms are mounted on a frame of four steel-bars, which are fixed on an aluminium ground plate. The total height of the apparatus is 1 250 mm.

4. Measuring conditions.

A transverse (or constant shear-) gradient appears when a fluid is confined between two parallel plates, one at rest and the other plate moving with constant velocity v_z due to the action of a constant external force (Fig. 3). This is the case of the plane Couette-flow and the gradient G can be written :

$$G = \frac{dv_z}{dx} [s^{-1}] \tag{1}$$

where x is the distance between the two plates.

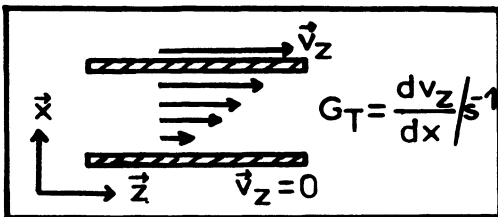


Fig. 3. — Transverse gradient between two parallel plates.

The laminar flow in the gap between two concentric cylinders, one of them rotating with a constant velocity U is in good approximation equal to the flow between two parallel plates, provided the gap-width is small compared with the diameter of the cylinders [2]. The shear gradient in this geometry is also supposed to be constant and can be connected with the rotation speed of the rotating cylinder :

$$G = \frac{2 \cdot \pi \cdot U \cdot R_a}{60 \cdot d} [s^{-1}] \tag{2}$$

where R_a is the inner radius of the rotor and d is the gapwidth. The torque exerted on the liquid in the gap and the shear force are a function of the viscosity of the system at a given shear-gradient. The range of operation of the apparatus is limited with regard to viscosity and shear gradient by several factors which

will be explained below. Figure 4 shows a double-logarithmic plot of the viscosity against the shear gradient for various operating parameters and illustrates under which conditions shear experiments can be performed.

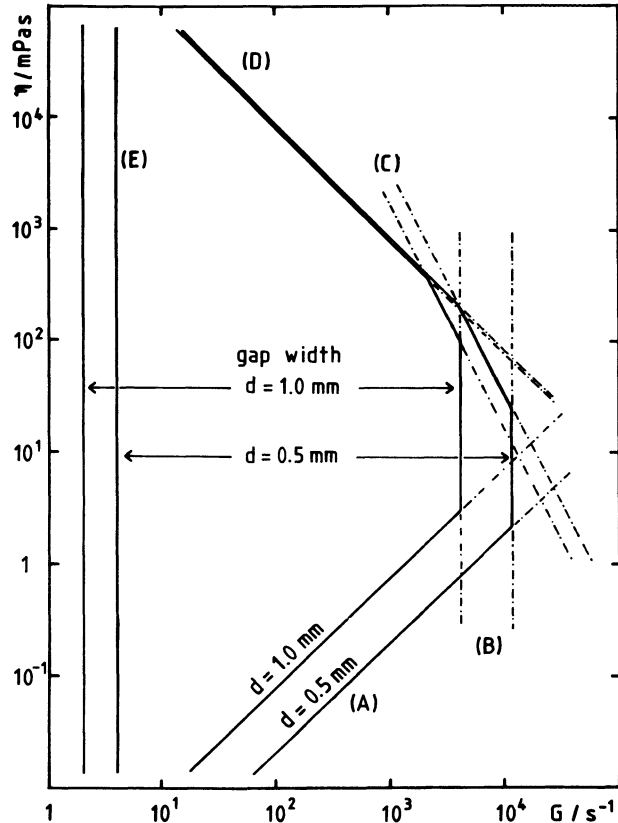


Fig. 4. — Operating range of the apparatus (see text). A : Transition laminar-turbulent flow. B : maximum ascent of the liquid in the gap. C : energy dissipation in the fluid. D : maximum torque of the motor. E : lowest stable motor speed.

4.1 TRANSITION LAMINAR-TURBULENT FLOW. — The measurements should be done in laminar flow for which it is necessary to estimate the transition to turbulence. The Reynolds number Re which characterizes this change laminar-turbulent in hydrodynamics, is given for the plane Couette-flow by (2) :

$$Re = \frac{\rho \cdot d^2 \cdot G}{\eta} \tag{3}$$

where ρ is the density in g/cm^3 , η is the viscosity in $g/(s \cdot cm)$, d is the gap-width in cm and G is the shear gradient in $1/s$. Different numerical values for Re can be found in the literature e.g. $Re = 1\,500$ [4] or $Re = 2\,000$ [2]. For smaller values of Re the transition to turbulent flow will occur at lower speeds. If we calculate with the most unfavourable value for the Reynolds number, $Re = 1\,500$, we can obtain

for the viscosity as a function of shear gradient G :

$$\eta_{\text{crit}} = f(G) = \frac{\rho \cdot d^2 \cdot G}{1500} \left[\frac{\text{g}}{\text{cm} \cdot \text{s}} \right]. \quad (4)$$

If the viscosity of the liquid system to be investigated is above that critical value, $\eta > \eta_{\text{crit}}$, laminar flow is expected. In figure 4, curve (A) shows the critical viscosity relation for the two possible gap-widths of the apparatus ; for the density a value of $\rho = 1 \text{ g/cm}^3$ has been used in the calculation.

4.2 ASCENT OF THE LIQUID IN THE GAP. — The gap between the two cylinders is open at the top and the solution will rise due to the action of the centrifugal force when one cylinder rotates. An approximative calculation yields for the difference of the meniscus between the wall of the inner cylinder and the wall of the outer cylinder Δz :

$$\Delta z \simeq \frac{G^2 \cdot d^3}{3 \cdot g \cdot R_a} [\text{cm}] \quad (5)$$

where $g = 981 \text{ cm/s}^2$. This relation is independent of the viscosity of the liquid. If we accept a value of $\Delta z_{\text{max}} = 2 \text{ cm}$ for the difference, the limit by ascent of the liquid for the highest attainable shear gradient is given by :

$$G_{\text{max}} = \left[\frac{2.3 \cdot g \cdot R_a}{d^3} \right]^{1/2} [\text{s}^{-1}]. \quad (6)$$

In figure 4 this is shown by curve (B) for the two possible gap-widths of the system.

4.3 LIMITATION BY THERMOSTAT CAPACITY. — The energy which is released when viscous liquids are sheared has to be removed in order to maintain a constant temperature. In the case of the shear apparatus the two compartments inside the stator are connected with an external thermostat. Provided that the dissipated heat is removed totally by the flow circuit through the stator, we can estimate from the maximum flowrate of the thermostat a limit for the temperature balance. The energy production in a sheared solution of viscosity η is given by :

$$P = \eta \cdot A \cdot d \cdot G^2 [\text{W}]. \quad (7)$$

It has to be removed by a cooling circuit :

$$P = \dot{n} \cdot c_p \cdot \Delta T [\text{W}] \quad (8)$$

where \dot{n} is the flow rate of the thermostat, c_p is the heat capacity of water ($c_p = 4.2 \text{ JK}^{-1} \text{ g}^{-1}$) and ΔT is the temperature difference in K. Therefore we obtain for the viscosity η_{crit} :

$$\eta_{\text{crit}} = f(G) = \frac{\Delta T \cdot c_p \cdot \dot{n}}{2 \pi \cdot R_a \cdot h \cdot d \cdot G^2} \left[\frac{\text{g}}{\text{cm} \cdot \text{s}} \right] \quad (9)$$

when substituting $A = 2 \pi \cdot R_a \cdot h$, where h is the filling height of the cylinder. With an experimentally determined flow rate $\dot{n} = 31 \text{ ml/s}$ this relation is shown in figure 4 by curve (C) for the two gap-widths of the apparatus and a temperature difference $\Delta T = 0.1 \text{ K}$. If the viscosity of the solution is below the critical value $\eta < \eta_{\text{crit}}$ the temperature of the solution in the gap should differ at most by $\Delta T = 0.1 \text{ K}$ from the temperature of the cooling liquid. It should be stated that the assumptions for this calculation are a) that the heat is removed totally from the stator and b) that the heat conduction through the quartz-glass wall is sufficient for our purpose.

4.4 LIMITATION BY THE TORQUE OF THE MOTOR. — If viscous liquids are sheared, the maximum torque of the motor will limit the speed and therefore we can estimate the highest attainable shear gradient. The relation between the torque of the motor D and the shear gradient G is given by :

$$D = \eta \cdot G \cdot A \cdot R_a [\text{dyn} \cdot \text{cm}] \quad (10)$$

where A is the sheared surface in cm^2 . The motor of our apparatus has a maximum torque of $D = 15 \text{ Ncm}$. So we can write for the critical viscosity η_{crit}

$$\eta_{\text{crit}} = f(G) = \frac{1}{G} \cdot \frac{15 \times 10^5}{A \cdot R_a} \left[\frac{\text{g}}{\text{cm} \cdot \text{s}} \right]. \quad (11)$$

If the viscosity of the liquid η is below this critical value the apparatus can be operated properly. In figure 4 this relation is shown by curve (D). An extension to higher viscosities is possible with another motor which is coupled with a gear.

4.5 LIMITATION BY LOWEST ROTATION SPEED OF THE MOTOR. — The lowest frequency for the rotation where the motor still runs stably has been determined for the three motors as $U \simeq 0.4 \text{ RPM}$. Applying equation (2) we get for the lowest attainable shear gradient :

$$G_{\text{min}} = \frac{2 \pi \cdot U \cdot R_a}{60 \cdot d} [\text{s}^{-1}]. \quad (12)$$

This is shown as curve (E) in figure 4.

5. Applications.

Typical systems which can be investigated by the apparatus are polymer solutions and melts, anisotropic biopolymers and viruses in solution and various colloidal liquids.

Preliminary results of measurements performed on highly diluted macromolecules show [5] that with this method a distortion of the equilibrium conformation by the shear gradient can be studied. A typical scattering pattern is shown in figure 5. Interesting features of these experiments are the Q -dependence of the ratio of the scattering intensity parallel to the

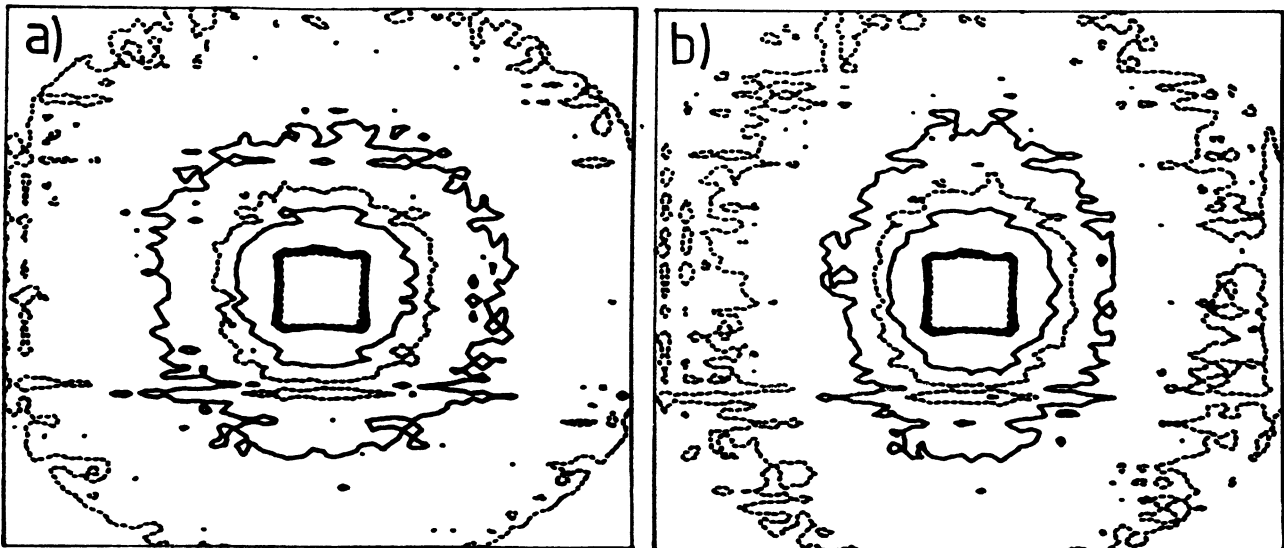


Fig. 5. — Uncorrected scattering pattern of a polystyrene-solution of $c = 6 \text{ mg/cm}^3$. a) at rest, b) in a shear gradient $G = 400 \text{ s}^{-1}$ ($\eta = 2 \text{ g/(cm s)}$).

flow direction to the isotropic scattering intensity (molecule at rest) and the behaviour of the observed anisotropy of the polymer coil with increasing shear gradient [6].

References

- [1] a) SCHMATZ, W., SPRINGER, T., SCHELLEN, J., IBEL, K., *J. Appl. Crystallogr.* **7** (1974) 96-116.
 b) IBEL, K., *J. Appl. Crystallogr.* **9** (1976) 296-309.
 [2] WIEGHARDT, K., *Theoretische Strömungslehre*. Stuttgart, 1965.
 [3] JANESCHITZ-KRIEGL, H., *Fortschr. Hochpolym.-Forsch.* **6** (1969) 170-318.
 [4] DE GENNES, P. G., *J. Chem. Phys.* **60** (1974) 5030.
 [5] OBERTHÜR, R. C., LINDNER, P., *Polymer Prepr.* **24**, 2 (1983) 419.
 [6] OBERTHÜR, R. C., LINDNER, P., to be published.